THE JOURNAL OF PHYSICAL CHEMISTRY C

Article

pubs.acs.org/JPCC

Atomistic Insights into Chemical Interface Damping of Surface Plasmon Excitations in Silver Nanoclusters

Oscar A. Douglas-Gallardo, Matías Berdakin, and Cristián G. Sánchez*

Departamento de Matemática y Física, Facultad de Ciencias Químicas, INFIQC-CONICET, Ciudad Universitaria, Universidad Nacional de Córdoba, X5000HUA Córdoba, Argentina

ABSTRACT: A detailed description of the mechanism underlying chemical interface damping (CID) in silver nanoclusters is presented. The effect of adsorbates on the surface plasmon excitation in silver nanoclusters is explored by means of a method based on time-dependent self-consistent charge density functional tight binding (TD-SCC-DFTB). By using this tool, we have calculated the homogeneous line width of the surface plasmon resonance (SPR) band for both naked and capped silver nanoclusters. A new picture explaining the decreased lifetime of the surface plasmon excitations is provided, in which coupling between particles states via adsorbate states enhances the natural dephasing mechanism of the surface plasmon excitation. To the best of our knowledge, this is the first report that addresses this topic from a fully atomistic time-dependent approach considering nanosized particles.

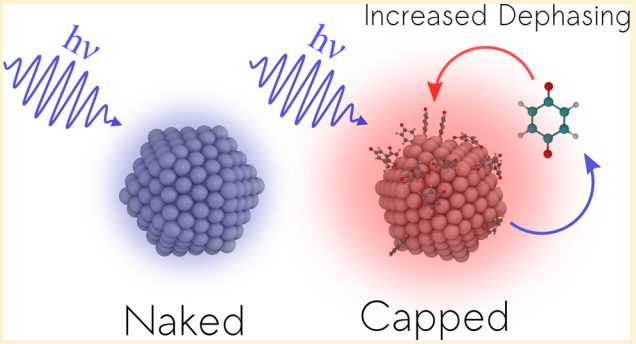

1. INTRODUCTION

Colloidal solutions of tiny noble metal particles often exhibit an intense optical absorption band located on the UV−vis region of the spectrum that arises from coherent oscillations of conductions electrons in response to external time-varying electric fields. This band is denominated the localized surface plasmon resonance (LSPR) band or simply surface plasmon resonance (SPR) band.[1,2] The excitation energy (E_{SPR}) and line width (Γ) of this band are its main spectroscopic features, and they depend strongly on size, shape, composition, and surrounding environment of the particles.[1,2] Both parameters are markedly modified when the size of the particles decreases (<10 nm) and complex size-related quantum and surface effects start to dominate the characteristics of the excitation. In this size regime the optical properties of metal noble nanocluster are still poorly understood due to the complex physical and chemical effects operating at these scales.[3] The spectroscopic changes are more noticeable in line width than excitation energy due to the surface and chemical scattering processes that take place in this size regime. The precise knowledge of the line width (and lifetime) of the SPR band is a very important aspect to note due to the many potential applications depending on it.[4−6] However, the experimental determination of SPR lifetimes presents some difficulties. The measurement of lifetime carried out by using time-resolved spectroscopic techniques is complicated due to the extremely fast dephasing time (1−10 fs) that characterizes surface plasmon excitations, particularly for smaller sizes.[5] Different terms contribute to the homogeneous line width (Γ) of the SPR band and are usually separated as an arithmetic sum:[6−8]

$$\Gamma = \gamma_b + \Gamma_{rad} + \Gamma_{e-s} + \Gamma_{CID} \quad (1)$$

The terms include the intrinsic bulk damping (γ_b), the radiative damping (Γ_{rad}), the damping due to electron−surface scattering (Γ_{e-s}), and the chemical interface damping (Γ_{CID}), originating from adsorbed chemical species.[9,10] The radiative damping is especially important for larger particles and negligible for sizes below 15 nm in the case of silver nanoparticles. The properties of the surface plasmon excitation are strongly modified by the chemical interface with the surroundings. The use of different molecules as capping agents becomes necessary to reach chemical and morphologic stability of particles.[11] The chemical interaction between the capping molecules and the surface modifies the position and line width of the SPR band. This phenomenon is known as chemical interface damping (CID), as mentioned above. The broadening of the SPR band is intimately related with the reduction of lifetime of the surface plasmon excitation and is especially relevant when the size of particles decreases.

The detailed electronic mechanism behind CID is not fully understood, and simple phenomenological models have been used to study its influence on the surface plasmon excitation. The first theoretical study that shed light on CID in small metal particles was performed by Persson in 1993.[10] This model proposes that the adsorbate-induced resonance states (or virtual levels) that occur close to the Fermi energy, due to adsorbate−substrate coupling, are responsible of the damping observed on the surface plasmon excitations. Hövel et al. extended this model by taking into account interband transitions in small noble metal particles.[12] Our group has

Received: August 23, 2016
Revised: September 30, 2016
Published: October 2, 2016

DOI: 10.1021/acs.jpcc.6b08519
J. Phys. Chem. C 2016, 120, 24389−24399

performed a study of this phenomenon using a simple model that considered the adsorbed molecule as a two-level system.[13] In this study two parameters were explored: the gap between the highest occupied molecular orbital−lowest unoccupied molecular orbital (HOMO−LUMO) of the adsorbate and the strength of the chemical binding between the adsorbate and the surface of the particle. We found that the interaction between the adsorbate and the surface induces shifting and broadening of the SPR band even in the weak coupling regime.

In this work we have studied the effect of adsorbates over the surface plasmon excitation in silver nanoclusters. The model used and the analysis provided enable us to reach a fully atomistic picture of CID from which the chemical contribution to the line width can be explained. Likewise, we have calculated line widths for both naked and capped silver nanoclusters. This is the first report that, to the best of our knowledge, surveys CID from a fully atomistic time-dependent description. Water and quinone have been chosen as capping molecules due to the fact that both molecules can be found within typical synthesis media used to produce silver nanoparticles in aqueous solutions. The choice of adsorbates presented in this work was made among a broader range for which a smaller set of screening simulations was performed. Since no significant differences in the underlying mechanism of the broadening were observed, we chose two examples which go from very weak damping to strong damping and focused on thoroughly analyzing the underlying dynamics of the damping process.

2. THEORETICAL METHOD

The electronic structure of the ground state (GS) for all studied systems was calculated using the self-consistent charge density functional tight binding (SCC-DFTB) method.[14] This approach is based on a controlled approximation of density functional theory (DFT) and has been successfully employed to describe the electronic structure of large organic and bioinorganic systems.[15,16] Specifically, we have used the DFTB + package,[17] which is an implementation of the SCC-DFTB method, to compute the GS Hamiltonian (H_{GS}), overlap matrix ($\mathbf{S}$), and the initial GS single-electron density matrix (ρ). The Hyb-0-2 DFTB parameter set[18,19] was employed in order to obtain the electronic structure and perform a geometry optimization of both naked and capped silver nanocluster. When optimizing the structure of capped silver nanocluster, only the molecular degrees of freedom were taken into account in order to minimize the increase in electron−surface scattering that adsorption may cause due to surface relaxation effects and isolate the influence of adsorbates purely on the electronic structure of the system. The total and partial density of states for these systems were calculated using the tool available (dp-tool) in the DFTB+ package.

The methodology applied to describe electronic dynamics of the whole system is based on the real-time propagation of the single-particle reduced density matrix (ρ) under the influence of an external time-varying potential (V_{ext}).

$$\hat{H}(t) = \hat{H}_{GS} + \hat{V}_{ext}(t) = \hat{H}_{GS} - E(t)\hat{\mu} \tag{2}$$

The Hamiltonian (H_{GS}) and overlap ($\mathbf{S}$) matrix obtained from the DFTB+ code are used as initial input to obtain the GS density matrix. The propagation of the density matrix is calculated through time integration of the Liouville−von Neumann equation of motion in the nonorthogonal basis

$$\frac{\partial\hat{\rho}}{\partial t} = \frac{1}{i\hbar}(\mathbf{S}^{-1}\hat{H}[\hat{\rho}]\hat{\rho} - \hat{\rho}\hat{H}[\hat{\rho}]\mathbf{S}^{-1}) \tag{3}$$

where $\mathbf{S}^{-1}$ is the inverse of the overlap matrix. Dirac δ pulses and sinusoidal time-dependent electric fields were used as external electric fields to perturb the whole system and obtain different dynamical information such as absorption spectra or resonance lifetimes. The method used is fully atomistic in the sense that all species are treated at the atomic level and all properties described stem from the used of a unique model for the electronic structure of the whole system, making no distinction between different species.

The optical absorption spectra for both naked and capped silver nanoclusters were obtained using as initial perturbation in the form of a Dirac δ pulse [$E(t) = E_0\delta(t - t_0)$, $E_0 = 0.001$ V/A]. Within the linear response regimen, when the applied electric field pulse is small, the dipole moment can be written as

$$\mu(t) = \int_{-\infty}^{\infty} \alpha(t - \tau)E(\tau)\, d\tau \tag{4}$$

where α is the time-dependent dynamic polarizability (or linear response function) along the axis over which the external field is applied. In frequency space the dynamic polarizability is related with the dipole moment through of the following expression:

$$\alpha(\omega) = \frac{\mu(\omega)}{E_0} \tag{5}$$

The absorption spectrum is proportional to the imaginary part of the frequency-dependent dynamic polarizability which can be calculated from the Fourier transform of the time-dependent dipole moment followed by the application of eq 4. In order to broaden the absorption band obtained from the electron dynamics before carrying out the Fourier transform of the time-dependent dipole moment its signal is damped within the simulation window using an exponential function with a time constant of 10 fs. This broadening is a technical necessity for the discrete Fourier transform to produce meaningful results for a finite (albeit long) dipole signal to reach a negligible value during the simulation window. This procedure broadens each and every spectral line uniformly by 0.033 eV. The broadening is an order of magnitude less than the spectral width of the SPR shown below. We have used the arithmetic average of frequency-dependent dynamic polarizability over the three Cartesian axes to calculate the absorption spectra for all studied systems.

In order to study the electron dynamics induced by resonant light absorption processes for both naked and capped silver nanoclusters, a sinusoidal time-dependent electric field in tune with the SPR band is used as external perturbation [$E(t) = E_0 \sin(\omega_{SPR}t)$]. This allows disclosure of the underlying dynamics that characterize the excited electron motion at frequency ω_{SPR}. It is important to stress that the time-dependent dipole moment in this type of simulation is not damped and constitutes a direct observable of the intrinsic microcanonical electronic dynamics of the system. Likewise, a deeper understanding of the nature of the excitations can be obtained from the molecular orbital populations dynamics following a laser excitation in tune with the excitation energy. The orbital populations can be calculated from the diagonal elements of the one-electron time-dependent density matrix transformed to the ground-state molecular orbital basis. Also, we have obtained molecular orbital shell populations by adding the contributions

DOI: 10.1021/acs.jpcc.6b08519
J. Phys. Chem. C 2016, 120, 24389−24399

coming from diagonal elements corresponding to each shell orbital.

The SCC-DFTB model used to describe the electronic structure of the whole system is a well-controlled approximation based on a second-order expansion of the exact DFT energy functional around a reference density. Our simulation method is an extension of SCC-DFTB to the time domain. This method has been used, and described, in the past by us,[15,16,20−27] and others, by propagating molecular orbitals instead of the single-particle density matrix[28] and in a linear response framework.[29] We have used the method to describe the absorption spectra of chlorophylls,[25,26] semiconductor nanoparticles,[20] graphene nanoflakes,[21] the dynamics of charge transfer in dye semiconductor nanoparticles,[15,16,24] even predicting new effects later confirmed by experiments,[24] the effect on the optical absorption spectra of DNA of intercalation compounds,[27] and charge transfer in donor−acceptor molecular complexes.[22]

3. RESULTS AND DISCUSSION

The optimized structures of all the systems studied within this work were obtained using the DFTB+ program package as described in the Theoretical Method section. Briefly, naked icosahedral silver nanoclusters structures were optimized without any restrictions to any atomic degree of freedom. In the case of capped silver nanoclusters, the geometry of the adsorbed molecules was fully optimized upon adsorption on the already obtained structures of naked silver nanoclusters. In the latter case, the degrees of freedom of silver atoms were kept frozen during the optimization. This was done to study the purely chemical contribution, independent of the structural disorder that surface relaxation may cause, which we already have identified in the past as a source of broadening.[30] As an outline of the present report, in section 3.1 we show the results from the simulation of absorption spectra of naked silver nanoclusters ranging from 1.1 to 3.3 nm (see structures in Figure 1).

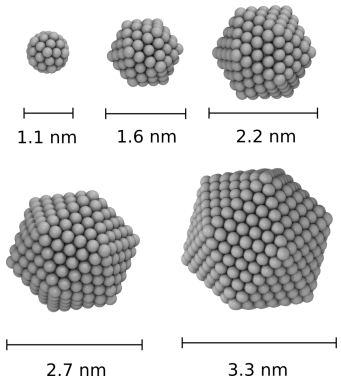

Figure 1. Schematic representation of the different silver nanocluster structures considered in this work; these structures contain 55, 147, 309, 561, and 923 silver atoms, following the natural progression of icosahedral face-centered cubic (fcc) structures.

Later on, within the same section, focus is placed on the electronic structure and photophysics underlying surface plasmon excitation properties of the naked Ag_{309} nanocluster which will set the ground to evaluate the influence of the capping molecules over the surface plasmon excitations response in section 3.2. The choice of this particle size is not arbitrary and is based on the necessity to establish a balance between studying a realistic nanosized system and the computational cost of the geometry optimization of capped nanoclusters.

3.1. Naked Silver Nanocluster. In nanoscopic scale, the face-centered cubic (fcc) crystalline structure of bulk silver is modified and different geometric isomers can be found. In the particular case of silver nanoclusters, the icosahedral form has been reported as the most stable crystalline structure up to 500 atoms.[3,31−33] In order to check the consistency of our model, structure optimization and energy calculations were performed for different geometric isomers using the DFTB+ program package, giving rise to the same conclusions (data not shown). From the obtained equilibrium structures the optical properties of different sizes of naked icosahedra silver nanocluster were studied; Figure 2a presents the obtained optical absorption spectra of Ag_{55}, Ag_{147}, Ag_{309}, Ag_{561}, and Ag_{923} nanoclusters.

For all sizes of particles considered the optical absorption spectrum is dominated by a single dipolar SPR band, even for the smallest particle size. As can be seen from Figure 2a, and in good agreement with previous theoretical and experimental reports,[1,2,33−37] as the size of the particle increases, both a red shift of the excitation energy [3.21 eV (Ag_{55}), 2.95 eV (Ag_{147}), 2.85 eV (Ag_{309}), 2.77 eV (Ag_{561}), 2.74 (Ag_{923}) eV] and an increase of the absorption intensity of the SPR band are observed. Furthermore, as shown in Figure 2b, and in agreement with previous reports,[30] the excitation energy associated with the SPR band exhibits a linear behavior with $N^{-1/3}$. The obtained intercept value of a linear regression of the plasmon resonance energy as a function of $N^{-1/3}$ is 2.42 eV (512 nm) and corresponds to the excitation energy reached in the limit when (1/radius) approaches to zero, that is, the limit of an infinitely large particle. Our results compare favorably with those presented in refs 38−41 that study particles of similar size (down to 1.5 nm). However, for the range of sizes presented here direct comparison with both experimental and theoretical results is difficult. First, experimental data on the silver dielectric constant that is used as input in all methodologies based on Mie theory exhibit an uncertainty significantly greater than gold experimental data.[42] This leads to an uncertainty in the SPR band peak position for silver. Likewise, when the size of particles is very small (<10 nm) these methodologies lose validity and the quantum-size-related effect should be taken into account. In this context, our work presents a very detailed study on the optical properties of silver nanocluster in a range of sizes outside the scope of both Mie theory and full TDDFT simulations. Second, it is very important to note that for nanostructures with size below to 5 nm the optical properties are still not completely understood and some controversy exists about the direction the SPR band peak positions shift with size.[3,43] Likewise, the formation of very small nanoparticles without the presence of capping agent is still experimentally very challenging, and therefore, no direct comparison with experimental data is possible yet. Taking into account the results presented so far, it can be stated that with the methodology employed in this work the main features of the absorption spectra (intensity and shape) of silver nanoclusters are recovered and the general trends expected as a function of the particle size are properly described.

A suitable characterization of the electronic properties of the naked silver nanocluster is required in order to understand the effect of adsorbates over the surface plasmon excitation in capped silver nanoclusters. In this sense, first, the electronic

DOI: 10.1021/acs.jpcc.6b08519
J. Phys. Chem. C 2016, 120, 24389−24399

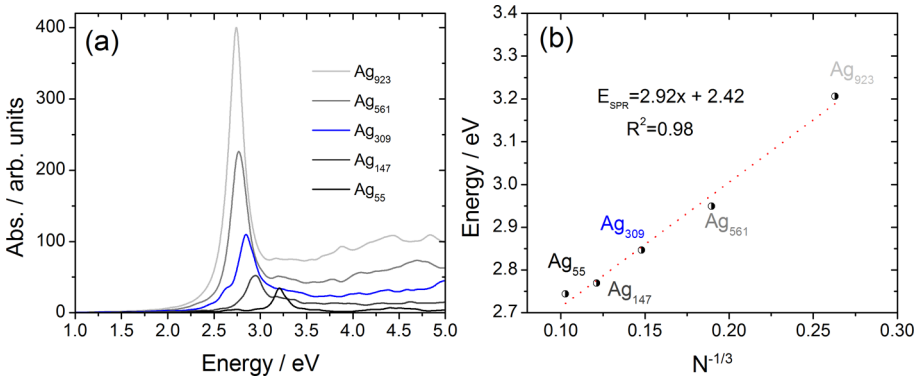

Figure 2. (a) Optical absorption spectra of naked icosahedral silver nanoclusters of different size. (b) Surface plasmon excitation energy as a function of the inverse cube root of the numbers of atoms together with a linear fit.

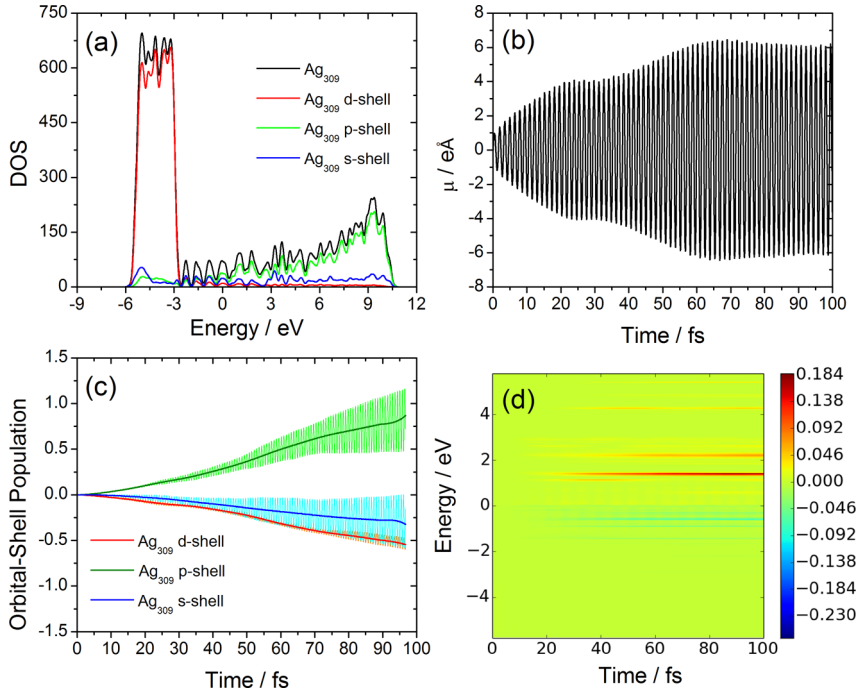

Figure 3. (a) Total density of states (black line) and projected (partial) density of states (pDOS) over different silver orbital shells (s shell, p shell, and d shell: colored lines). (b) Dipole moment and electron orbital population dynamics resulting from continuous light irradiation at the SPR band (2.85 eV) for a naked silver nanocluster of 309 atoms, discerned by (c) shell and (d) energy.

structure of a naked Ag_{309} nanocluster was analyzed through the calculation of its density of states (DOS) and projected (or partial) density of states (pDOS), Figure 3a. The DOS can be separate in two principal bands, a d band and the sp band. The d band is mainly composed by silver d-shell states (Figure 3a, red line) and is located 4 eV below the Fermi level. On the other hand, the sp band is composed from both contributions of silver s-shell and p-shell states (Figure 3a, blue and green lines). It is important to note that the conduction part of the sp band stems from unoccupied electronic states that are mainly provided by silver p-shell states. Figure 3b shows the dipole moment resulting from light absorption processes of Ag_{309} nanocluster.

In order to gain insight into the photophysical processes that arise during light absorption, the electronic dynamics of naked silver nanocluster was studied by tuning the frequency of an applied sinusoidal time-dependent electric field with the excitation energy of the SPR band corresponding to the Ag_{309} structure (2.85 eV, blue line in Figure 2a). Two different but complementary analyses were obtained from electronic dynamics associated with the light absorption process: first, electron orbital shell (OS) population dynamics, which provides a dynamical picture of the change in the population of atomic shells normalized to the ground-state population during light absorption (Figure 3c), and second, the electron orbital energy (OE) population analysis shown in Figure 3d, that is a transformation of the population analysis to the energy domain. This last analysis allows us to locate the occupied/unoccupied states involved in the absorption process in the DOS picture and the time evolution of their occupations.

As can be seen from Figure 3c, the excitation of the SPR band produces a population transfer from s-shell and d-shell to p-shell states. This result can be understood as the promotion of electrons from d,s shells to unoccupied states of the p shell. A complementary picture can be obtained through the (OE) population dynamics shown in Figure 3d. The main change occurs within the s,p band in the energy region that spans between ±2 eV from the Fermi level. Although the dynamics

DOI: 10.1021/acs.jpcc.6b08519
J. Phys. Chem. C 2016, 120, 24389−24399

triggered by light absorption exhibits a complex behavior, it is important to state that the analysis presented here provides a transparent picture of the photophysics underling SPR response. The combination of the information provided in Figure 3 points to the fact that the SPR band is caused by the promotion of electrons from occupied states of the s,p band to unoccupied states of the same band. Nevertheless, in the energy range between −2 eV and the Fermi energy, the contribution of states from the silver d shell is not negligible, and is overlapped with the s,p band. This is why Figure 3c shows that part of the depopulation of the valence band is originated from d-shell orbitals. Despite this, it is important to note that the d-shell states involved in the SPR response are not those that form the bulk of the d band. Although this difference may seem subtle at first glance, it is a fundamental piece of the description of the photophysics of the SPR, because it is already known that in the case of silver nanocluster the interband transition associated with electron promotion from d band to sp band does not strongly affect the optical features associated with the SPR band.[7,10,44] From observation of the time evolution of the dipole moment signal two regimes can be observed. The signal first grows and saturates, and a second process occurs after 40 fs causing a new growth of the dipole signal and a second saturation regime at higher values. The population analysis in Figure 3, parts c and d, clearly shows that the cause of the second saturation process occurs due to the promotion of d states which is delayed in time with respect to s electrons. This can be appreciated in the curvature changes in the time-evolving populations in Figure 3c and the population of new (initially empty) states around 40 fs that can be clearly seen in Figure 3d. The two sequential processes observed in Figure 3b can be accounted for by the fact that there are two distinct excitations present at the energy upon which illumination proceeds: the plasmon excitation and an interband transition. These two processes have different cross sections and dampings; this explains the delay in the d excitation which has a lower cross section. Other effects such as the influence of an enhanced local field may aid the excitation of the interband transition due to nonlinearities.

3.2. Capped Silver Nanocluster. Water and quinone molecules have been selected as model adsorbates to study the effect of capping agents over the surface plasmon excitation. The selection of these adsorbates is grounded on two main reasons: First, both molecules represent suitable models of adsorbates that can be found in typical synthesis procedures.[34,45−49] Water is the universal solvent used in wet synthetic methods. On the other hand, hydroquinone has been used as an effective weak reducing agent in different strategies to achieve control on rate formation of silver particles.[34,45−49] When this synthetic approach is employed, quinone remains in solution as the oxidized form of hydroquinone. Second, because water and quinone present different chemical bonding with silver surfaces, the employment of these molecules allows us to explore the effect of bond characteristics on the optical response of the SPR in a capped nanocluster.

Structures used to study the optical properties of capped silver nanoclusters were obtained as described in the Theoretical Method section and are shown for two representative cases in Figure 4.

The optical absorption spectra of both w-Ag_{309} and q-Ag_{309} with different numbers of adsorbed molecules are shown in Figure 5, parts a and b, respectively.

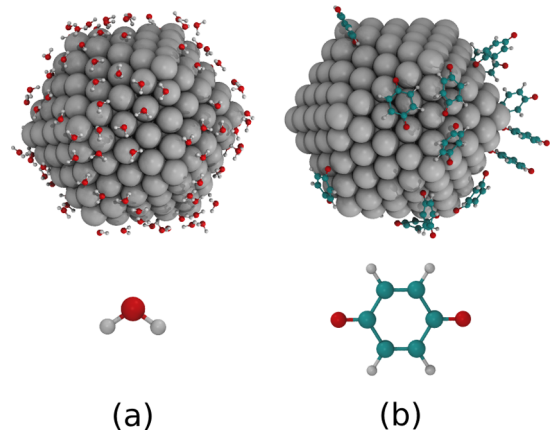

Figure 4. Optimized structures of representative examples of both systems studied: (a) w-Ag_{309}; (b) q-Ag_{309}. The systems shown in the figure have 123 and 16 adsorbates in each case.

In both cases the main spectroscopic features are modified when the number of adsorbed molecules increases. As expected from previous experimental and theoretical reports,[3,10,12,50−52] these changes are characterized by a red shift and a marked broadening of the peak associated with the SPR band. It can be clearly observed that the modifications are more pronounced in the case of quinone. The difference between the effects of both adsorbates can be understood on the basis of the type of chemical bonding established with the silver surface.

The dipole moment is a direct emergent of electronic dynamics and was used to determine the line width and lifetime of the SPR band for both naked and capped silver nanoclusters. In order to obtain an analytical expression that relates the dipole moment response with the line width, a model was adopted for the time-dependent dynamic polarizability

$$\alpha(t;\Gamma) = k_1\left[\exp\left\{\frac{-\Gamma t}{2}\right\}\sin\{\Omega t\}\right]\theta(t) \tag{6}$$

where $\theta(t)$ is the Heaviside function. In this model we have assumed a single resonance (Ω) with a lifetime of (Γ) and provide a good description of the dynamics of the SPR for the capped particles studied here.

In the linear response regime, the dipole moment is related to the applied electric field and time-dependent dynamic polarizability through eq 4, and the analytic expression that connects the time-dependent dipole moment and line width is

$$\mu(t;\Gamma) = -k_1E_0\left\{k_2\cos(\Omega t)\left\{\exp\left(\frac{-\Gamma t}{2}\right) - 1\right\} + k_3\sin(\Omega t)\left\{\exp\left(\frac{-\Gamma t}{2}\right) + 1\right\}\right\} \tag{7}$$

From eq 7 it can be seen that, upon constant illumination, the dipole moment oscillates in time (due to the cos and sin factors), and grows in time, with a decreasing speed caused by the exponential factors. The picture provided by eq 7 fully accounts for the dynamics of the peak dipole moment shown in Figure 5, parts c and d. It is important to note that the dipole moment is damped by two exponential functions that depend only on the line width within this model. If we consider only the exponential functions, leaving out the trivial oscillatory component, this last equation can be re written as

DOI: 10.1021/acs.jpcc.6b08519
J. Phys. Chem. C 2016, 120, 24389−24399

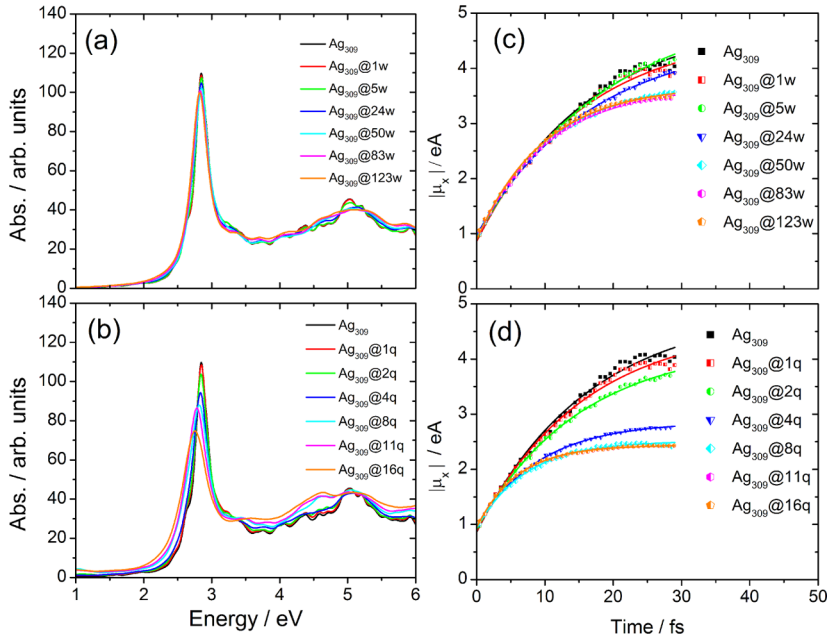

Figure 5. Optical absorption spectra of a Ag_{309} nanocluster with different amounts of adsorbed molecules (a) H_2O and (b) quinone. Panels c and d show the absolute value of the peak of the dipole moment on the *x*-direction and its respective fitting curve for both H_2O and quinone, respectively.

$$\Lambda(t;\Gamma) = \left\{k_4\left\{\exp\left(\frac{-\Gamma t}{2}\right) - 1\right\} + k_5\left\{\exp\left(\frac{-\Gamma t}{2}\right) + 1\right\}\right\} \tag{8}$$

where k_1, k_2, k_3, k_4, and k_5 are constants independent of Γ, related to the absorption coefficient and field strength. Then, in order to obtain the line width associated with spectra shown in Figure 5, parts a and b, the maxima of the absolute value of the time-dependent dipole moment obtained from electronic dynamics upon constant illumination in resonance with the plasmon was fitted to eq 8 as shown in Figure 5, parts c and d. The obtained values of line width and the position of the peaks associated with the SPR band are shown in Figure 6. It can be clearly appreciated from the figure that the effect of quinone on both the red shift and broadening is much larger than that for water.

As noted before for the case of naked particles, the dipole signal shows two clearly distinguishable relaxation regimes, a fact that was explained by the delay in the involvement of d electrons in the excitation. For the fitting procedure detailed in the preceding paragraph only the first relaxation process was used. This decision is based on the fact that the second process is significantly reduced upon increasing the number of adsorbates and is nonexistent for particles with more than four adsorbates. These effects of adsorbates on the participation of d electrons on the excitation are explained below.

The results obtained from the fitting of the time-dependent dipole moment with eq 8 follow the trends shown in Figure 5, parts a and b, regarding the broadening of the SPR band as the amount of adsorbate molecules increase, and are in good agreement with previous reports.[3,10,12,50−52] It is clearly observed in Figure 6a that the extent of the broadening produced by the absorption of quinone is significantly higher than the one produced by water. Once the line width is obtained, the lifetime associated with the homogeneous broadening of the SPR band can be calculated from eq 9:[9]

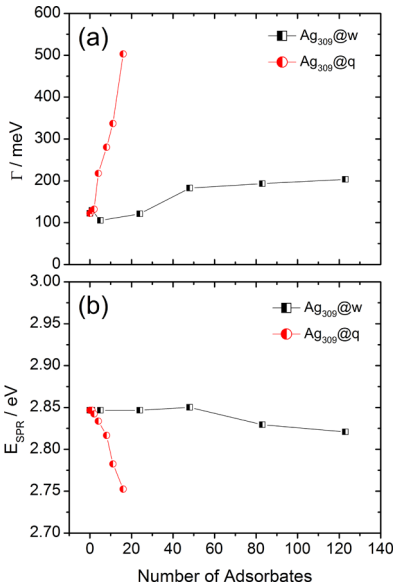

Figure 6. (a) Homogeneous line width corresponding to the SPR band obtained from electronic dynamics and (b) excitation energy associated with the SPR band for both systems, as a function of number of adsorbed molecules.

$$\Gamma = \frac{2\hbar}{T_2} \tag{9}$$

The results obtained are summarized in Table 1.

In the naked particle the dephasing is present, but since the number of states involved is relatively small, the dephasing time is larger than for the capped particle and so is the excitation lifetime. The method used in this work takes into account the bulk damping, electron−surface scattering, and CID on exactly the same grounds. Only the global, all-encompassing damping is obtained from the simulation. All of its contributions are emergents of the simulated electronic dynamics upon light absorption. As detailed in the Theoretical Method section we

DOI: 10.1021/acs.jpcc.6b08519
J. Phys. Chem. C 2016, 120, 24389−24399

Table 1. Capping Effect over the SPR Band

water				quinone			
C.M.[a]	E_{SPR}/eV[b]	Γ/meV[c]	T_2/fs[d]	C.M.[a]	E_{SPR}/eV[b]	Γ/meV[c]	T_2/fs[d]
0	2.85	122	10.8	0	2.45	122	10.8
1	2.85	129	10.2	1	2.85	129	10.2
5	2.85	105	12.5	2	2.84	132	10.0
24	2.85	121	10.9	4	2.83	218	6.1
48	2.85	183	7.2	8	2.82	281	4.7
83	2.83	193	6.8	11	2.78	337	3.9
123	2.82	203	6.5	16	2.75	503	2.6

[a]C.M. stands for the number of capping molecules over the silver nanoclusters. [b]Peak position of the SPR band. [c]Corresponds to the homogeneous line width obtained by means of eq 8. [d]Corresponds to the corresponding lifetime from the homogeneous line width obtained by means of eq 9.

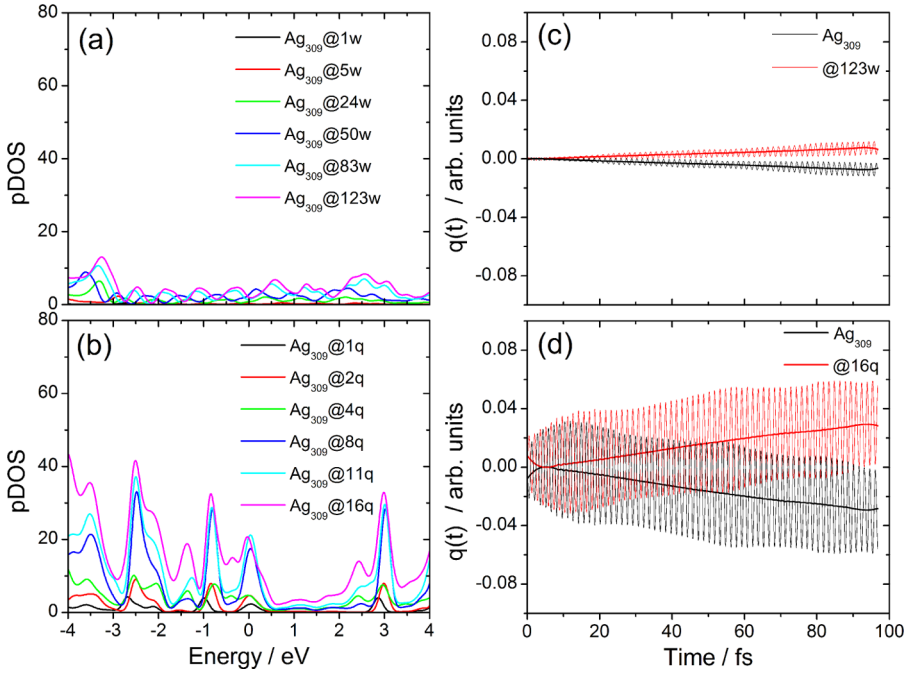

Figure 7. Projected density of states (black line) over capping molecules as a function of number of adsorbate for both systems (a) w-Ag_{309} and (b) q-Ag_{309}. Difference of Mulliken charges over both parts of the systems silver cluster and capping agent for both systems (c) 123w-Ag_{309} and (d) 16q-Ag_{309}. The two sets of lines in panels c and d arise from the bare charge in each part of the system (highly oscillating curves) and the running average over an oscillating period in tune with the resonance for the case of the slowly varying lines.

have maintained the atomic structure of the particles frozen to their equilibrium structure in all simulations, purposefully neglecting surface relaxation upon adsorption in order to minimize the interference between electron−surface scattering and CID. This makes the electron−surface contribution to the scattering the same (at least at the level of structural modifications) for both naked and capped particles and allows us to obtain conclusions on the underlying causes for CID as emergents of the changes in electronic dynamics.

In order to explore the causes for the observed CID, first the effect over the electronic energy landscape introduced by the interaction with the capping agent was studied. Figure 7, parts a and b, shows the pDOS over the capping moiety near Fermi energy for both 123w-Ag_{309} and 16q-Ag_{309}. The chemical interaction between capping and silver nanocluster results in the modification of the electronic structure of whole system.

Comparison between parts a and b of Figure 7 shows that quinone adds more states near the Fermi level than the water molecule; this difference can be understood in terms of the nature of the chemical bond resulting from the interaction between the capping agent and the silver nanocluster surface.[8] When a covalent chemical bond is established between the capping agent and the cluster, as is the case for quinone, the electronic structure is markedly altered. We expect these modifications to be more important for other adsorbates which adsorb with higher adsorption energies reflecting on the strength of the bonding. A stronger bond with the adsorbate would imply larger changes to the electronic structure of the cluster. However, at this point, with the available data at hand no clear-cut correlation between parameters such as adsorption energy and damping can be made; this will be the object of future work. It is important to note that the orientation of water molecules adsorbed over the silver surface resembles the structure proposed by Sánchez[53] where water molecules are adsorbed parallel to the surface. This orientation allows an effective interaction between water molecule and the metal surface through the oxygen lone pair.

In order to shed light into the mechanism that relates the above-described modification in the electronic structure and the CID, the photophysics underling light absorption was studied. For this purpose, time-dependent Mulliken charge differences with respect to the ground-state charges over both silver cluster

DOI: 10.1021/acs.jpcc.6b08519
J. Phys. Chem. C 2016, 120, 24389−24399

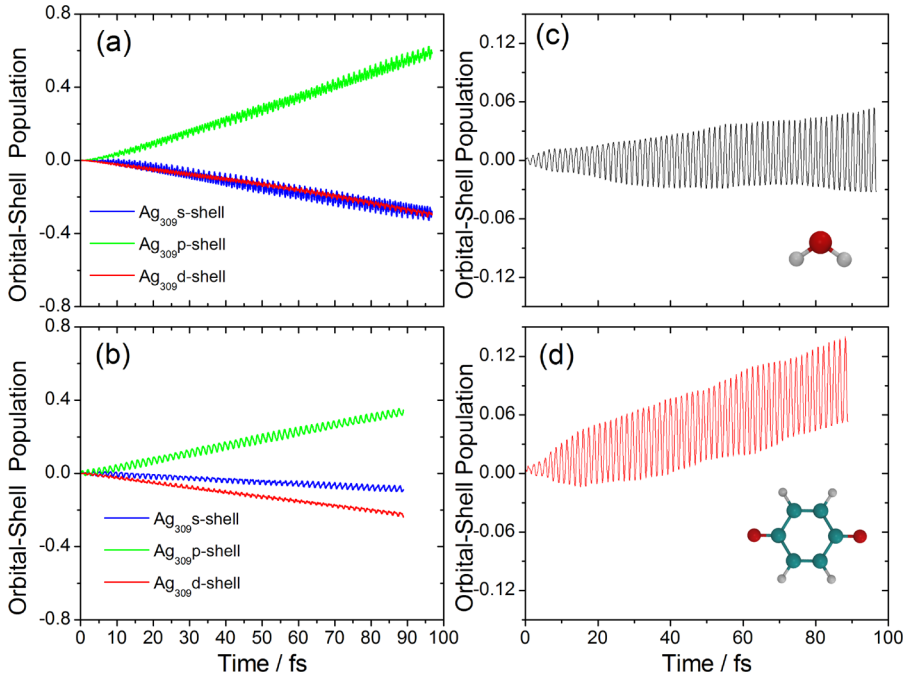

Figure 8. Dynamic change on electron orbital shell population under continuous laser illumination corresponding to a silver cluster of 309 atoms with capping to both system (a) H_2O and (b) quinone. Electron orbital shell population dynamic changes under laser illuminations corresponding to capping to both systems (c) H_2O and (d) quinone.

and capping moieties were recorded for 123w-Ag_{309} and 16q-Ag_{309}, and are shown in Figure 7, parts c and d, respectively. In both cases a net negative charge transfer is observed from the silver particle to the capping moieties, but in the case of quinone the extent of this charge transfer is larger. The metal−adsorbate charge transfer described here may be described as a coherent spatially indirect transition taking electrons from the metal to the molecule. This behavior is closely related with the difference between the chemical interaction of both capping agents and the silver nanoclusters already mentioned and can be understood with atomistic detail in terms of the orbital shell dynamic picture shown in Figure 8.

In the quinone case, when examining the OS population dynamics in the nanocluster moiety, Figure 8b, it can be seen that the injection of electronic population in the p shell of the silver nanocluster is noticeably reduced in comparison with the population reached for the same shell when water-capped (Figure 8a) or naked particles (Figure 3c) are considered. This can be understood in combination with the charge-transfer process to the capping moiety described in Figure 7, considering that a fast process occurs that drains electronic population from silver p-shell states to unoccupied states of the capping molecules. This idea is verified when the OS dynamic population of the capping molecules is considered, Figure 8, parts c and d. Concomitantly with the larger charge transfer observed for quinone in Figure 7d, Figure 8d clearly shows that light irradiation induces population transfer to the p-shell orbital from quinone oxygen atoms. This process can be rationalized if we take into account the hybridization change of the carbonyl group of quinone that occurs when the molecule interacts with the surface, weakening the doubly bound C−O and leaving a p orbital available to be occupied. In the case of water, this hybridization change is not possible, and consequently, the p-shell population in the corresponding silver nanocluster resembles the corresponding population of the naked particle. The charge transfer to adsorbates upon illumination in resonance with the SPR band is a consequence of the mixing between particle states and adsorbate states which causes charge to leak from excited particle states into unoccupied adsorbate states linearly with time (this process was observed for the case of dyes adsorbed on semiconductor).[15,16]

A dynamical picture of the excitation process is completed when time-dependent electronic state population dynamics is analyzed. Figures 3d and 9, parts a and b, present the time-dependent population of each state, as a function of the state energy and time for naked, water-capped, and quinone-capped particles, respectively.

It can be seen from Figure 3d that for the naked particle the electronic excitation remains constrained in two well-localized manifolds of states. In the opposite way it is clearly seen that in the case of quinone (Figure 9b) the interaction with the capping molecules delocalizes the electronic excitation in a manifold of states that span a wider energy range. This delocalization of the electronic excitation is promoted by the new states added by the capping molecule near the Fermi level and produces the loss of coherence of electron oscillation and the subsequent decay of the lifetime and broadening of the SPR band. The new states are not important in the population that themselves carry upon excitation, which, as is clear from Figure 8, is small. These new states produce coupling between cluster states that were nonexistent in the naked particle. The spread of the excitation over a larger manifold of states, facilitated by the new channels offered by adsorbates states, is the cause for the rapid decoherence. This adsorbate-induced delocalization in energy and coupling is also the cause of the change in time evolution of the dipole signal upon constant illumination. As mentioned above, for the case of naked particles, two excitation processes with a time delay between them are observed for that case. As can be seen from Figure 8, parts a and b, in the case of

DOI: 10.1021/acs.jpcc.6b08519
J. Phys. Chem. C 2016, 120, 24389−24399

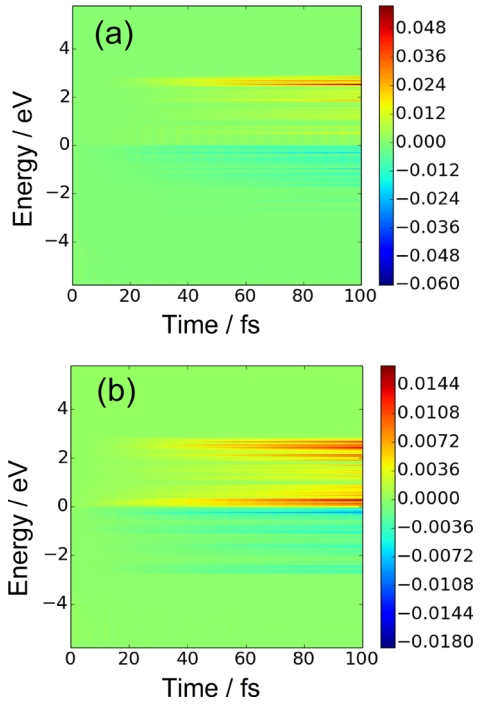

Figure 9. Electronic dynamic over illumination laser: (a) 309@123w; (b) 309@16q.

capped particles the excitation of d electrons starts synchronously with that of s electrons.

Understanding the nature of the excitations that are involved upon light absorption from a dynamical perspective needs to be made with the aid of new tools. This is the purpose of the picture supplied by Figures 8 and 9. These provide a purely dynamical picture, grounded on the equilibrium electronic structure energy spectrum and classification of the orbital character of electrons promoted in energy. It is important to stress that, due to the fact that the system is nonperiodic, no band structure can be constructed. No inferences stemming from selection rules involving momentum conservation can be made either given the fact that the system is finite; a change of picture is needed, and it is the aim of the present work to provide such picture. Furthermore, even if we included all of the states and energies that form the eigenvalue spectrum of the static Hamiltonian, the dynamical excitation process mixes these states dramatically given the fact that they are very close in energy. The advantage of a dynamical perspective is that it allows us to describe the excitation in a global way without having to resort to the eigenvalue spectrum alone, and the rather limiting concept of individual electronic transitions.

Plasmon excitations are characterized by their collectiveness, by precisely the fact that they represent the effect of a strongly coherent superposition of many individual excitations. The broadening of plasmon excitations occurs by the natural dephasing of this superposition, a process known as Landau damping.[54] In the extreme case of a particle−hole excitation in a molecule, for example, a single energy (and therefore frequency) participates; in this case, continuous laser illumination causes long-lived Rabi oscillations that do not decay, unless coupling to the environment is included, and an ever-increasing dipole moment linear in time if the excitation is within the linear response regime is observed upon constant illumination.[26] In the case of collective excitations, the superposition of many frequencies causes the dipole signal representing the added results of many individual oscillations that eventually dephase; this dephasing is presented as a flattening in the resulting dipole moment signal upon constant illumination. In the naked particle the dephasing is present, but since the number of states involved is relatively small, the dephasing time is large and so is the excitation lifetime. The coupling of cluster states via a covalently bound adsorbate, as clearly seen in Figure 9, increases the number of states participating in the excitation, drastically increasing the dephasing and decoherence of the plasmon. More complex effects than the mere damping of plasmon oscillations (such as the appearance of new combined plasmon−molecule excitations) are possible in regimes outside of the scope of the present work, when the adsorbate HOMO−LUMO transition is close to the plasmon energy. These systems are difficult to realize experimentally with silver nanoparticles which often present absorption in the outset of the visible range (>400 nm) of the spectrum. These effects have been studied by us in the past by using a much more simplified model of the electronic structure.[13]

4. CONCLUSIONS

We have presented a detailed study of the effect of adsorbates on surface plasmon excitations in silver nanocluster by describing the electronic dynamics within the time-dependent self-consistent charge density functional tight binding (TD-SCC-DFTB) model. We have found that changes on spectroscopic features of the SPR band can be understood by the effect of coupling between particle states provided by the adsorbate. The chemical interaction between the adsorbate molecules and nanocluster surface produces an electronic reorganization that modifies the excitation dynamics of the SPR band. This reorganization is caused by coupling of states present in the particle that otherwise would not participate in the excitation. Likewise, the presence of these states reduces the lifetime of the SPR excitation, therefore producing a broadening the SPR band by enhancing the natural mechanisms of plasmon dephasing. We have also calculated the line width of the SPR band for both naked and capped silver nanocluster through modeling the time evolution of the dipole moment of the particle upon continuous illumination. The values obtained are in good agreement with previous work. To the best of our knowledge, this is the first work that performs an atomistic study of chemical interface damping with significant coverage of realistic adsorbates providing a detailed quantum dynamical picture of chemical interface damping.

AUTHOR INFORMATION

Corresponding Author

*E-mail: cgsanchez@fcq.unc.edu.ar. Phone: +54-351-5353850, ext 55020.

Notes

The authors declare no competing financial interest.

ACKNOWLEDGMENTS

The authors acknowledge financial support by Consejo Nacional de Investigaciones Científicas y Técnicas (CONICET) through Grant PIP 112-201101-0092 and wish to thank SeCyT for the funding received. This work has used computational resources from CCAD (Universidad Nacional de Córdoba (http://ccad.unc.edu.ar), in particular Mendieta Cluster, which is part of SNCAD-MinCyT, República

DOI: 10.1021/acs.jpcc.6b08519
J. Phys. Chem. C 2016, 120, 24389−24399

Argentina. O.A.D.-G. and M.B. wish to thank CONICET for their postdoctoral fellowships.

REFERENCES

(1) Khlebtsov, N. G.; Dykman, L. A. Optical Properties and Biomedical Applications of Plasmonic Nanoparticles. *J. Quant. Spectrosc. Radiat. Transfer* **2010**, *111*, 1−35.

(2) Coronado, E. A.; Encina, E. R.; Stefani, F. D. Optical Properties of Metallic Nanoparticles: Manipulating Light, Heat and Forces at the Nanoscale. *Nanoscale* **2011**, *3*, 4042−4059.

(3) Peng, S.; McMahon, J. M.; Schatz, G. C.; Gray, S. K.; Sun, Y. Reversing the Size-Dependence of Surface Plasmon Resonances. *Proc. Natl. Acad. Sci. U. S. A.* **2010**, *107*, 14530−14534.

(4) Hendrich, C.; Bosbach, J.; Stietz, F.; Hubenthal, F.; Vartanyan, T.; Träger, F. Chemical Interface Damping of Surface Plasmon Excitation in Metal Nanoparticles: A Study by Persistent Spectral Hole Burning. *Appl. Phys. B: Lasers Opt.* **2003**, *76*, 869−875.

(5) Sönnichsen, C.; Franzl, T.; Wilk, T.; von Plessen, G.; Feldmann, J.; Wilson, O.; Mulvaney, P. Drastic Reduction of Plasmon Damping in Gold Nanorods. *Phys. Rev. Lett.* **2002**, *88*, 077402.

(6) Olson, J.; Dominguez-Medina, S.; Hoggard, A.; Wang, L.-Y.; Chang, W.-S.; Link, S. Optical Characterization of Single Plasmonic Nanoparticles. *Chem. Soc. Rev.* **2015**, *44*, 40−57.

(7) Link, S.; El-Sayed, M. A. Shape and Size Dependence of Radiative, Non-Radiative and Photothermal Properties of Gold Nanocrystals. *Int. Rev. Phys. Chem.* **2000**, *19*, 409−453.

(8) Link, S.; El-Sayed, M. A. Optical Properties and Ultrafast Dynamics of Metallic Nanocrystals. *Annu. Rev. Phys. Chem.* **2003**, *54*, 331−366.

(9) Hartland, G. V. Optical Studies of Dynamics in Noble Metal Nanostructures. *Chem. Rev.* **2011**, *111*, 3858−3887.

(10) Persson, B. N. J. Polarizability of Small Spherical Metal Particles: Influence of the Matrix Environment. *Surf. Sci.* **1993**, *281*, 153−162.

(11) Daniel, M. C. M.; Astruc, D. Gold Nanoparticles: Assembly, Supramolecular Chemistry, Quantum-Size Related Properties and Applications toward Biology, Catalysis and Nanotechnology. *Chem. Rev.* **2004**, *104*, 293−346.

(12) Hövel, H.; Fritz, S.; Hilger, A.; Kreibig, U.; Vollmer, M. Width of Cluster Plasmon Resonances: Bulk Dielectric Functions and Chemical Interface Damping. *Phys. Rev. B: Condens. Matter Mater. Phys.* **1993**, *48*, 18178−18188.

(13) Negre, C. F. A.; Sánchez, C. G. Effect of Molecular Adsorbates on the Plasmon Resonance of Metallic Nanoparticles. *Chem. Phys. Lett.* **2010**, *494*, 255−259.

(14) Elstner, M.; Porezag, D.; Jungnickel, G.; Elsner, J.; Haugk, M.; Frauenheim, T.; Suhai, S.; Seifert, G. Self-Consistent-Charge Density-Functional Tight-Binding Method for Simulations of Complex Materials Properties. *Phys. Rev. B: Condens. Matter Mater. Phys.* **1998**, *58*, 7260−7268.

(15) Oviedo, M. B.; Zarate, X.; Negre, C. F. A.; Schott, E.; Arratia-Pérez, R.; Sánchez, C. G. Quantum Dynamical Simulations as a Tool for Predicting Photoinjection Mechanisms in Dye-Sensitized TiO2 Solar Cells. *J. Phys. Chem. Lett.* **2012**, *3*, 2548−2555.

(16) Negre, C. F. A.; Fuertes, V. C.; Oviedo, M. B.; Oliva, F. Y.; Sánchez, C. G. Quantum Dynamics of Light-Induced Charge Injection in a Model Dye-Nanoparticle Complex. *J. Phys. Chem. C* **2012**, *116*, 14748−14753.

(17) Aradi, B.; Hourahine, B.; Frauenheim, T. DFTB+, a Sparse Matrix-Based Implementation of the DFTB Method. *J. Phys. Chem. A* **2007**, *111*, 5678−5684.

(18) Szücs, B.; Hajnal, Z.; Frauenheim, T.; González, C.; Ortega, J.; Pérez, R.; Flores, F. Chalcogen Passivation of GaAs(1 0 0) Surfaces: Theoretical Study. *Appl. Surf. Sci.* **2003**, *212−213*, 861−865.

(19) Szücs, B.; Hajnal, Z.; Scholz, R.; Sanna, S.; Frauenheim, T. Theoretical Study of the Adsorption of a PTCDA Monolayer on S-Passivated GaAs(1 0 0). *Appl. Surf. Sci.* **2004**, *234*, 173−177.

(20) Fuertes, V. C.; Negre, C. F. A.; Oviedo, M. B.; Bonafé, F. P.; Oliva, F. Y.; Sánchez, C. G. A Theoretical Study of the Optical Properties of Nanostructured TiO_2. *J. Phys.: Condens. Matter* **2013**, *25*, 115304.

(21) Wettstein, C. M.; Bonafé, F. P.; Oviedo, M. B.; Sánchez, C. G. Optical Properties of Graphene Nanoflakes: Shape Matters. *J. Chem. Phys.* **2016**, *144*, 224305.

(22) Medrano, C. R.; Oviedo, M. B.; Sánchez, C. G. Photoinduced Charge-Transfer Dynamics Simulations in Noncovalently Bonded Molecular Aggregates. *Phys. Chem. Chem. Phys.* **2016**, *18*, 14840−14849.

(23) Negre, C. F. A.; Perassi, E. M.; Coronado, E. A.; Sánchez, C. G. Quantum Dynamical Simulations of Local Field Enhancement in Metal Nanoparticles. *J. Phys.: Condens. Matter* **2013**, *25*, 125304−125314.

(24) Negre, C. F. A.; Young, K. J.; Oviedo, M. B.; Allen, L. J.; Sánchez, C. G.; Jarzembska, K. N.; Benedict, J. B.; Crabtree, R. H.; Coppens, P.; Brudvig, G. W.; et al. Photoelectrochemical Hole Injection Revealed in Polyoxotitanate Nanocrystals Functionalized with Organic Adsorbates. *J. Am. Chem. Soc.* **2014**, *136*, 16420−16429.

(25) Oviedo, M. B.; Sánchez, C. G. Transition Dipole Moments of the Qy Band in Photosynthetic Pigments. *J. Phys. Chem. A* **2011**, *115*, 12280−12285.

(26) Oviedo, M. B.; Negre, C. F. A.; Sánchez, C. G. Dynamical Simulation of the Optical Response of Photosynthetic Pigments. *Phys. Chem. Chem. Phys.* **2010**, *12*, 6706−6711.

(27) Primo, E. N.; Oviedo, M. B.; Sánchez, C. G.; Rubianes, M. D.; Rivas, G. A. PT NU. *Bioelectrochemistry* **2014**, *99*, 8−16.

(28) Niehaus, T. A.; Heringer, D.; Torralva, B.; Frauenheim, T. Importance of Electronic Self-Consistency in the TDDFT Based Treatment of Nonadiabatic Molecular Dynamics. *Eur. Phys. J. D* **2005**, *35*, 467−477.

(29) Niehaus, T. A.; Suhai, S.; Della Sala, F.; Lugli, P.; Elstner, M.; Seifert, G.; Frauenheim, T. Tight-Binding Approach to Time-Dependent Density-Functional Response Theory. *Phys. Rev. B: Condens. Matter Mater. Phys.* **2001**, *63*, 085108.

(30) Negre, C. F. A.; Sánchez, C. G. Atomistic Structure Dependence of the Collective Excitation in Metal Nanoparticles. *J. Chem. Phys.* **2008**, *129*, 034710.

(31) Baletto, F.; Mottet, C.; Ferrando, R. Microscopic Mechanisms of the Growth of Metastable Silver Icosahedra. *Phys. Rev. B: Condens. Matter Mater. Phys.* **2001**, *63*, 155408.

(32) Baletto, F.; Mottet, C.; Ferrando, R. Freezing of Silver Nanodroplets. *Chem. Phys. Lett.* **2002**, *354*, 82−87.

(33) Jensen, L. L.; Jensen, L. Atomistic Electrodynamics Model for Optical Properties of Silver Nanoclusters. *J. Phys. Chem. C* **2009**, *113*, 15182−15190.

(34) Pérez, M. A.; Moiraghi, R.; Coronado, E. A.; Macagno, V. A. Hydroquinone Synthesis of Silver Nanoparticles: A Simple Model Reaction To Understand the Factors That Determine Their Nucleation and Growth. *Cryst. Growth Des.* **2008**, *8*, 1377−1383.

(35) Toscano, G.; Straubel, J.; Kwiatkowski, A.; Rockstuhl, C.; Evers, F.; Xu, H.; Mortensen, N. A.; Wubs, M. Resonance Shifts and Spill-out Effects in Self-Consistent Hydrodynamic Nanoplasmonics. *Nat. Commun.* **2015**, *6*, 7132.

(36) Kooij, E. S.; Ahmed, W.; Zandvliet, H. J. W.; Poelsema, B. Localized Plasmons in Noble Metal Nanospheroids. *J. Phys. Chem. C* **2011**, *115*, 10321−10332.

(37) Majhi, J. K.; Mandal, A. C.; Kuiri, P. K. Theoretical Calculation of Optical Absorption of Noble Metal Nanoparticles Using a Simple Model: Effects of Particle Size and Dielectric Function. *J. Comput. Theor. Nanosci.* **2015**, *12*, 2997−3005.

(38) Cottancin, E.; Celep, G.; Lermé, J.; Pellarin, M.; Huntzinger, J. R.; Vialle, J. L.; Broyer, M. Optical Properties of Noble Metal Clusters as a Function of the Size: Comparison between Experiments and a Semi-Quantal Theory. *Theor. Chem. Acc.* **2006**, *116*, 514−523.

(39) Raza, S.; Stenger, N.; Kadkhodazadeh, S.; Fischer, S. V.; Kostesha, N.; Jauho, A.-P.; Burrows, A.; Wubs, M.; Mortensen, N. A. Blueshift of the Surface Plasmon Resonance in Silver Nanoparticles Studied with EELS. *Nanophotonics* **2013**, *2*, 131−138.

DOI: 10.1021/acs.jpcc.6b08519
J. Phys. Chem. C 2016, 120, 24389−24399

(40) Raza, S.; Kadkhodazadeh, S.; Christensen, T.; Di Vece, M.; Wubs, M.; Mortensen, N. A.; Stenger, N. Multipole Plasmons and Their Disappearance in Few-Nanometre Silver Nanoparticles. *Nat. Commun.* **2015**, *6*, 8788.
(41) Scholl, J. A.; Koh, A. L.; Dionne, J. A. Quantum Plasmon Resonances of Individual Metallic Nanoparticles. *Nature* **2012**, *483*, 421−427.
(42) Johnson, P. B.; Christy, R. W. Optical Constants of the Noble Metals. *Phys. Rev. B* **1972**, *6*, 4370−4379.
(43) Mogensen, K. B.; Kneipp, K. Size-Dependent Shifts of Plasmon Resonance in Silver Nanoparticle Films Using Controlled Dissolution: Monitoring the Onset of Surface Screening Effects. *J. Phys. Chem. C* **2014**, *118*, 28075−28083.
(44) Pinchuk, A.; Kreibig, U.; Hilger, A. Optical Properties of Metallic Nanoparticles: Influence of Interface Effects and Interband Transitions. *Surf. Sci.* **2004**, *557*, 269−280.
(45) Moiraghi, R.; Douglas-Gallardo, O. A.; Coronado, E. A.; Macagno, V. A.; Pérez, M. A. Gold Nucleation Inhibition by Halide Ions: A Basis for a Seed-Mediated Approach. *RSC Adv.* **2015**, *5*, 19329−19336.
(46) Gentry, S. T.; Kendra, S. F.; Bezpalko, M. W. Ostwald Ripening in Metallic Nanoparticles: Stochastic Kinetics. *J. Phys. Chem. C* **2011**, *115*, 12736−12741.
(47) Wang, H.; Chen, D.; Wei, Y.; Yu, L.; Zhang, P.; Zhao, J. A Localized Surface Plasmon Resonance Light Scattering-Based Sensing of Hydroquinone via the Formed Silver Nanoparticles in System. *Spectrochim. Acta, Part A* **2011**, *79*, 2012−2016.
(48) Morasso, C.; Picciolini, S.; Schiumarini, D.; Mehn, D.; Ojea-jiménez, I.; Zanchetta, G.; Vanna, R.; Bedoni, M.; Prosperi, D.; Gramatica, F. Control of Size and Aspect Ratio in Hydroquinone-Based Synthesis of Gold Nanorods. *J. Nanopart. Res.* **2015**, *17*, 330−337.
(49) Li, J.; Wang, W.; Zhao, L.; Rong, L.; Lan, S.; Sun, H.; Zhang, H.; Yang, B. Hydroquinone-Assisted Synthesis of Branched Au−Ag Nanoparticles with Polydopamine Coating as Highly Efficient Photothermal Agents. *ACS Appl. Mater. Interfaces* **2015**, *7*, 11613−11623.
(50) Charlé, K.-P.; Frank, F.; Schulze, W. The Optical Properties of Silver Microcrystallites in Dependence on Size and the Influence of the Matrix Environment. *Berichte der Bunsengesellschaft für Phys. Chemie* **1984**, *88*, 350−354.
(51) Charlé, K. P.; Schulze, W.; Winter, B. The Size Dependent Shift of the Surface Plasmon Absorption Band of Small Spherical Metal Particles. *Z. Phys. D: At., Mol. Clusters* **1989**, *12*, 471−475.
(52) Rekha, T. N.; Umadevi, M.; Rajkumar, B. J. M. Structural and Spectroscopic Study of Adsorption of Naphthalene on Silver. *Mol. Phys.* **2015**, *113*, 3673−3682.
(53) Sánchez, C. G. Molecular Reorientation of Water Adsorbed on Charged Ag(1 1 1) Surfaces. *Surf. Sci.* **2003**, *527*, 1−11.
(54) Kreibig, U.; Vollmer, M. *Optical Properties of Metal Clusters*; Springer Series in Materials Science 25; Springer: Berlin Heidelberg, Germany, 1995.

DOI: 10.1021/acs.jpcc.6b08519
J. Phys. Chem. C 2016, 120, 24389−24399